



Research article



The Deposition by Raffaello Sanzio: New analytical insights on old cross sections for the characterisation of pictorial palette

Marcella Ioele^{a, **}, Alessandro Ciccola^{b, *}, Paolo Postorino^c^a Istituto Centrale per il Restauro, via di San Michele 25, 00153, Roma, Italy^b Dip. di Biologia Ambientale, Sapienza Università di Roma, piazzale Aldo Moro 5, 00185, Roma, Italy^c Dip. di Fisica, Sapienza Università di Roma, piazzale Aldo Moro 5, 00185, Roma, Italy

ARTICLE INFO

Keywords:

Raffaello Sanzio
Painting palette
SEM-EDX
Raman
SERS

ABSTRACT

In 2020, 500th anniversary of Raffaello Sanzio death, his *Deposition* (1507), -the altarpiece known also as the *Pala Baglioni*, today located at the Borghese Gallery in Rome-has been subjected to conservative revision and preventive conservation project. This included in-depth diagnostic campaigns through most modern non-invasive techniques, together with the analysis of old cross sections from the same Pala. These latter, prepared between 1966 and 1972, preserved in ICR laboratory of chemistry and testing materials archive, have been used to deepen the knowledge of Raffaello painting techniques. The use of such cross sections was fundamental to verify the original pictorial film and restoration re-paintings before the conservation intervention in the same years.

In this paper, the results of analytical insights on Raffaello pictorial palette are presented. The information is obtained by the analysis of the old ICR stratigraphic sections, through the use of Scanning Electron Microscope with Energy Dispersive X-Ray analysis (SEM-EDX) and micro-Raman (632.8 nm), while Surface Enhanced Raman Scattering (SERS) analysis through colloidal paste has been tested for the identification of organic lake-pigments present in low concentration and for the successful recognition of copper resinate, whose SERS spectrum is here reported for the first time, according to our knowledge. This combined diagnostic approach has made it possible to recognize the pigments employed in the different pictorial layers, such species in traces and those from organic materials, responding to open questions arising previous non-invasive analyses and highlighting further aspects of the illustrious master refined painting technique.

1. Introduction

In 2020, commemorating the 500th anniversary of Raffaello's death, a comprehensive study was carried out to deep into the painter's pictorial technique. This work involved an extensive diagnostic campaign, conducted on all Raffaello's works housed in the Borghese Gallery of Rome. The *Deposition*, the altarpiece painted in 1507, also known as the *Pala Baglioni*, located at the Borghese Gallery (Fig. 1a), has been submitted to a conservative revision and preventive conservation project, supported by a new campaign of

* Corresponding author.

** Corresponding author.

E-mail address: alessandro.ciccola@uniroma1.it (A. Ciccola).

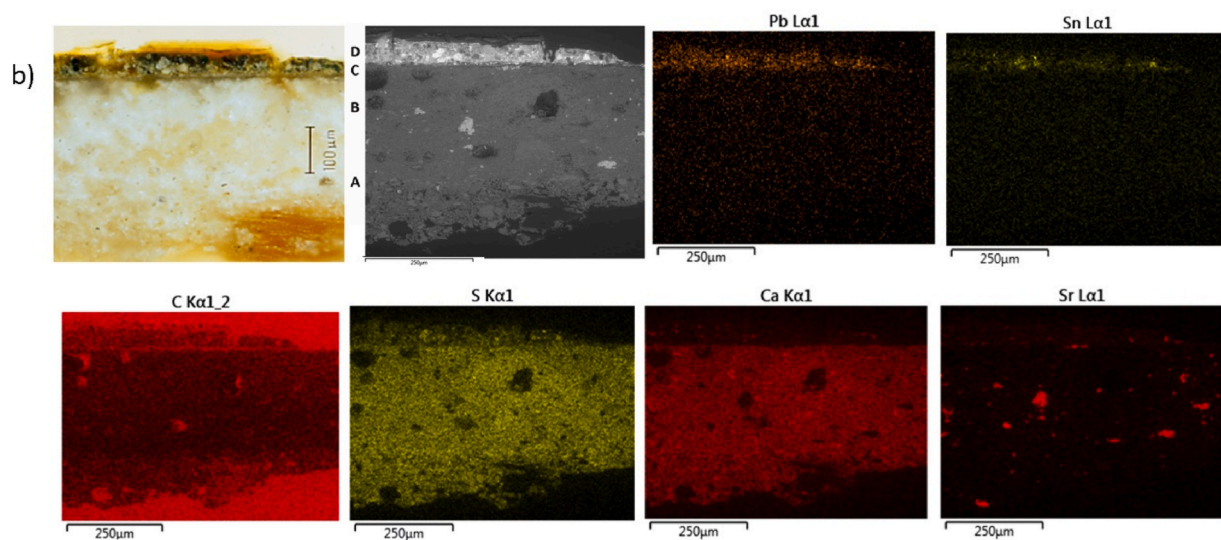


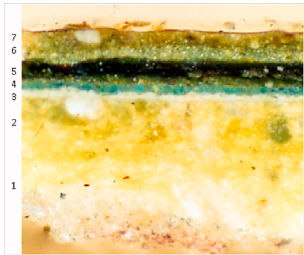
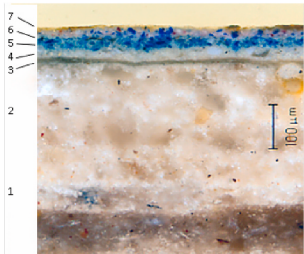

Fig. 1. The *Deposition*, before restoration intervention of 2020 (a). Section 1132; optical microscope and SEM image (BSE), X-ray maps for lead, tin, carbon, sulfur, calcium and strontium (b).

investigations using modern non-invasive techniques [1,2]. This was the last one of a series of non-invasive diagnostic campaigns, which have allowed extending progressively the knowledge about the materials used by the painter for this masterpiece [3–14]. Since its creation, actually, the *Deposition* was subjected to several restoration interventions, among which some are documented: the first known intervention in 1875, by Luigi Lais, was followed by some fixing operations of detached fragments in 1914, 1935, 1936. Between 1966 and 1972, a restoration intervention was conducted on the same Pala by the Istituto Centrale per il Restauro (ICR), followed in 2004–2005 by cleaning operations on the aged varnish and by the 2020 intervention. Proper diagnostic campaigns corresponded to some among these operations: the first two XRF analyses took place in the 1966–1972 restoration [4] and, separately, in 1984 [8]. In 1995 radiography and further XRF measurements were conducted, while several non-invasive spectroscopies were applied during 2004–2005 [3,9–14]. Finally, in the above-mentioned 2020 intervention, Macro X-Ray Fluorescence (MA-XRF) and hyperspectral imaging were used [1,2,7]. However, with reference to some limitations of the non-invasive techniques, a micro-invasive analysis appeared to be necessary to fully clarify the pigments composition and complete the overall portrait of Raffaello's materials and techniques. Though, for ethical reasons, the collection of new samples was avoided, and it was decided to address the analyses on the old cross sections, prepared between 1966 and 1972, during the related restoration intervention conducted by ICR. This approach represents an interesting and sustainable proof of concept, which shows how the application of new techniques to old cross-section could extend the amount of information achievable.

The ICR laboratory of chemistry and testing materials archive conserves more than 8000 cross sections prepared in the last 70 years of activity, during restoration intervention of works by the most illustrious Italian and world masters of painting. In the perspective of a sustainable diagnostic approach, ICR archive represents an extremely stimulating library from which new studies could kick off [15], as in this case. During ICR restoration, between 1966 and 1972, twenty-four stratigraphic sections were prepared from the *Deposition*. Some diagnostic investigations were carried out, relating to the study of Raffaello pictorial technique, but only with the instrumental facilities available at the time, such as microscope analyses and micro-chemical tests [4]. Even if that set of data resulted extremely useful for the conservation intervention at that time, the analytical methods and sensitivity today available open to new scenarios, thus offering the possibility of deepening our knowledge on Raffaello's work from these stratigraphic sections from the 1960s. These represent, indeed, an interesting and useful document for reconstructing the precious painting conservation history, as they constitute a "photograph" of the situation of the original pictorial film and, moreover, of the restoration re-paintings before intervention of

Table 1

Cross section from ICR archive analysed between 2020 and 2023.

N° cross section (<i>date</i>) Area of sampling	Original images of the cross section (1966–1971)	Analysis	Reading of the cross section and materials identified from below
1131 (1967) Green dress of Grifonetto Baglioni, between the legs of Christ		2020 OM SEM-EDX 2021–23 Micro-Raman SEM-EDX insights	1° preparatory layer <i>gesso grosso</i> containing celestine, 2° preparatory layer <i>gesso fine</i> containing celestine, 3° yellowish organic waterproofing layer, 4° whitish <i>imprimitura</i> containing lead white, <i>giallolino</i> and grinded glass 5° green layer (three paint brushes) containing malachite, <i>giallolino</i> and lead white 6° first overpainting layer containing copper resinate, lead white, <i>giallolino</i> 7° second overpainting layer containing copper resinate, lead white, calcium carbonate and copper sulfates
1522 (1969) Iridescent blue drapery of the female figure on the right		2020 OM SEM-EDX 2021–23 Micro-Raman Raman SERS, SEM-EDX insights	1° preparatory layer <i>gesso grosso</i> containing celestine, 2° preparatory layer <i>gesso fine</i> containing celestine, 3° yellowish organic waterproofing layer 4° whitish <i>imprimitura</i> containing lead white, <i>giallolino</i> and grinded glass 5° first blue paint layer containing lead white, azurite, iron oxides, litharge, and green earth 6° second blue paint layer containing lead white, lapis lazuli iron oxides and red lake, 7° organic (varnish) layer
1517 (1969) green ground under Nicodemus' foot, along the first crack on the left		2020 OM SEM-EDX 2021–23 Micro-Raman SEM-EDX insights	1° preparatory layer <i>gesso grosso</i> containing celestine, 2° preparatory layer <i>gesso fine</i> containing celestine, 3° yellowish organic waterproofing layer, 4° whitish <i>imprimitura</i> containing lead white, <i>giallolino</i> and grinded glass 5° dull green paint layer containing lead white, malachite, <i>giallolino</i> , litharge and iron oxides, possible presence of a red lake 6° organic (varnish) layer

1966–1972.

In 2020, fourteen of the twenty-four sections from the *Deposition* stored in the ICR archive -considered representative of several painted areas-were analysed by Scanning Electron Microscopy coupled to Energy Dispersive X-ray Spectroscopy (SEM-EDX). In the sections studied (Table 1; Table 1S in Supplementary Material), analyses evidenced pigments coherent with those available at the time, such as lead white, lead-tin yellow, lapis lazuli, bone black, iron oxides, copper containing pigments (e.g.: azurite, malachite [5,6]). The presence of copper resinate was presumed in repainting layers over green paint layers. In addition to the above-mentioned pigments, non-invasive analyses evidence the presence of gold, cinnabar, red lake, umber earth [7].

Following this study, with the aim of providing more information on the composition of the pictorial palette of Raffaello, the combined approach of SEM-EDX and micro-Raman analysis was chosen to integrate and complete the characterization about the original and restoration pigments present in the cross-sections from the *Deposition*. The two techniques, in fact, result complementary in providing different typologies of information (elemental for SEM-EDX, molecular for Raman): their combination allows a solid identification of pigments in the stratigraphic layers and lets to confirm or reject preliminary hypotheses based on non-invasive techniques. Moreover, with reference to the investigated cross-sections and their date of production, the application of these techniques results in a clear advancement and information enrichment, providing both confirming and novel data.

Among the fourteen cross-sections coming from the *Deposition* analysed in 2020, three were selected for Raman analysis. Extensive analysis was not performed on all of them, as some of the sections were partially or remarkably damaged due to the execution in 1972 of micro-chemical tests for the characterization of the binders. For instance, section 1567 (Table 1S) showed a noticeable darkening all over the main layers, due to the Graaf test for the identification of proteins, while SEM-EDX had evidenced a diffuse presence of copper, which could not be attributed only to the pigments but also to the residues of the test reactive. In this case, the molecular Raman analysis would have been difficult to perform, time-consuming and not informative. Moreover, as observable in Table 1S, for some sections SEM-EDX analysis provided a complete characterization of the pigments, especially by comparison with published data coming from previous non-invasive campaigns [3–14].

For this reason, the Raman analysis was focused only on three historical cross-sections. Despite the restricted number of these samples could limit the abstraction to the pictorial technique of the artist, the selected cross-sections are more complex from the stratigraphic point of view, and they were not seriously undermined by previous micro-chemical tests. These cross-sections were also indicative of painted areas, for which previous non-invasive and SEM-EDX analyses did not solve all the doubts about the composition and/or the stratigraphy of the pigments, while the information about the chemical data deriving from the study of these cross-sections in the original report [4] was extremely limited. In particular, with reference to open analytical questions, the following cross-section were selected.

- 1131: this is the only cross-section from Grifonetto's dress, which was not subjected to Graaf test (Table 1S). For this area, SEM-EDX and the non-invasive analyses could not provide the specific identification of the green pigment, but just detected the presence of copper, which is common to several species of this color [3,7], even if some indirect conclusions are addressed on the base of trace elements and impurities. Regarding previous studies on the cross-section, the original report [4] does not provide exhaustive experimental data, so the identification of the green pigments represented an analytical issue to solve and this cross-section was selected for Raman analysis.
- 1522: this cross-section presents some red particles likely attributable to a red lake, with reference to the previous SEM-EDX and non-invasive campaigns. Cross section 1522 was chosen for molecular analytical insights, since elemental analysis alone could not give information about pigments employed to create the purple shades on the blue. In particular, even if the use of several red lakes was assessed in the painting [7,13,14], for this area this was uncertain, because no specific pattern attributable to this organic species was identified, maybe for its low concentration and the absorption interference of other pigments, like azurite. Finally, the cross-section presented a double blue layer, in agreement with other cross-sections from other areas (e.g. 955 and 994; Table 1S), so it was considered representative of the other ones in order to confirm the hypothesis of an inner layer of azurite and an upper one in lead white and ultramarine, coming from previous investigations [3–7,13,14]. The molecular analysis of this cross-section was considered helpful in providing new data, consequently.
- 1517: this cross-section is indicative of the green ground under Nicodemo's foot. It has been selected instead of 1132, because, even if most of the morphological and elemental characteristic of pigment particles are homogeneous and comparable in the two sections, for 1517 the *imprimitura* layer is clearly evident, where particles probably related to lead tin yellow (*giallolino*) were observable. Moreover, it showed some Al-rich red particles, indicative of an organic lake. From this point of view, the comparison of Raman data from this section with those obtained from 1131 and from 1152 could provide complete details about the present copper-base and lake pigments, also with reference to the above-mentioned open analytical issues [3–7,13,14].

In this paper we present some new analytical insight performed on these chosen stratigraphic sections by the combined use of SEM-EDX and micro-Raman with 632.8 nm laser excitation. Details about the preparatory layers are also provided, with reference to section 1132 but coherent for all the samples. Moreover, Surface Enhanced Raman Scattering (SERS) data are provided, which opened new perspectives from the analytical point of view. These better performing techniques allowed to complete the reading of the stratigraphy and to obtain more in-depth and specific information about the materials present in the preparatory and in each pictorial layer, if compared to the data coming from previous study of the same samples [4,5], where it was not possible to obtain molecular information. The study of historical cross-section with new techniques, with reference to their realization, allowed to highlight further aspects of Raffaello painting technique, especially in terms of selected materials, completing and integrating the studies conducted so far [1–14]. This type of approach could be easily transferred to other historical archives, and, in the case of Raffaello's painting, it

represents a new step towards further research by means of more specific and innovative methodologies.

2. Materials and methods

2.1. Optical microscope (OM) analysis of stratigraphic sections

Old stratigraphic sections have an altered appearance, turning yellow-brown due to the inevitable aging phenomena both of the englobing resin and of the Canada balm placed over the section under the coverslip. On the selected sections, after removing the slide, the balm layer was gently removed with a swab soaked in isopropanol. In some cases, it was necessary to re-polish the section with very light abrasive paper. It is fundamental to highlight that no information about the specific location of the samples was provided in the original analysis report [4], but only to the general painting area, where they were collected (e.g.: green dress of Grifonetto Baglioni, Fig. 1S), so we are able to refer only to these data.

The stratigraphic polished sections were observed with a Leitz DM RXP microscope in reflected visible and UV light. Images were taken with a Leica MC190 HD digital camera and Leica Image 1000 image acquisition software. For the observations in UV fluorescence (50W Hg HBO lamp) a type A filter was used (BP excitation filter 340–380 nm, dichromatic foil 400 nm, barrier filter LP425).

2.2. SEM-EDX

SEM-EDX analyses were performed with a Zeiss EVO 60 model scanning electron microscope (EP-SEM) with a lanthanum hexaboride filament (acceleration voltage up to 30 KV), equipped with an OXFORD Inca Pentaflex EDS elemental analysis microprobe (EDX) for semi-quantitative analysis. The measurements were performed operating at 20 KV, in low pressure mode (100 Pa) on the cross-sections, without carrying out metallization. The images were recorded with the backscattered electron detector (BSE). The instrument is equipped with AZtecEnergy management software.

2.3. Raman and SERS analyses

Raman and SERS analyses were performed on a Horiba Jobin-Yvon HR-Evolution micro-Raman setup, equipped with a 632.8 nm laser and a motorized XY Mapping Stage.

The standard Raman analysis was performed on different points of the exposed area of the cross-sections. Set conditions for the spectra acquisition were varied from point to point of the sample in order to maximize the signals and they involved: 50X or 100× magnification, laser intensity of 0.38–7.50 mW, accumulation time of 30 s maximum for scan, 60 scans maximum. For all the samples, Raman spectra presented a fluorescence background, whose interference did not hinder the identification of the highest intensity peaks. However, in order to highlight the presence of further signals, a polynomial fit and consequent subtraction of the fitted baseline were applied (polynomial degree: 9) through the LabSpec software tool. A light smoothing was applied to decrease the spectral noise and to facilitate the individuation of the main frequencies. For these aims, the software Origin9 was used (Adjacent-Averaging method, points of window: 5).

For the SERS analysis, Ag-colloidal pastes were prepared adapting the procedure already described in the literature [16]. In brief, Ag-colloids were prepared following Leopold and Lendl methodology [17]: two solutions, one containing 0.021 g of $\text{NH}_2\text{OH HCl}$ in 5 mL of MilliQ water and the other one with 0.02 g of NaOH in 5 mL of MilliQ water, were added to a solution of 0.017 g of AgNO_3 in 90 mL of MilliQ water under gentle magnetic stirring to induce the formation of colloids. Then, 50 μl of a solution of MgSO_4 0.01 M were added to 4 mL of Ag-colloids and the dispersion was centrifuged for 20 min at 9500 rpm (temperature: 5 °C) and the supernatant was removed. Afterwards, colloidal pastes were applied on to the cross-section surface, in an area previously selected after microscopic observation, using a Pasteur pipette and left drying (4 h). SERS spectra were acquired in correspondence of Ag clusters in proximity of points/area of interest, previously identified on the cross-sections by comparison with optical and SEM-EDX images, in order to take into account of potential issues of reproducibility related to interaction of the analytes with the nanoparticles. At least three spectra were collected for every area of interest. Set conditions for the SERS spectra acquisition were changed from point to point of the sample in order to maximize the signals and they involved: 50X or 100× magnification, laser intensity of 0.15–0.75 mW, accumulation time of 3 s maximum for scan, 60 scans maximum.

The points in the cross-sections corresponding to Raman and SERS analyses are provided in Table 2S (Supplementary Materials) on SEM images for a clearer identification, and they are identified by a proper legend corresponding to the related spectra (in the same document). For the interpretation of Raman spectra and their assignation, the individuation of the highest intensity bands represented the initial step for the attribution on the base of comparison with the literature (spectra acquired at the same wavelength were preferred, if available) and with spectra of reference standards. Taking into account of the complexity of the matrices, generally the lower intensity bands were used to confirmed the assignations if they could be considered observable (signal/noise >3, at least). In some cases, some bands, which could not fulfil the signal/noise criterion but resembling bands present in literature, were cited for clarity of the reader. Noticeable variations (e.g.: broadness) in the experimental spectra with respect to the literature ones were highlighted in the discussion.

3. Results

3.1. Preparatory layers

On all the fourteen sections analysed in 2020 through SEM-EDX, a double preparatory plaster layer was found, the first with coarser gypsum particle size (*gesso grosso*), the second with thinner and more compact (*gesso fino*), both in a protein binder.¹ Gypsum contains strontium sulphate (celestine) inclusions with granulometry varying from a few microns up to a few tens of microns (see for example section 1132, Fig. 1b). Over preparatory layer, in most of the sections, a thin organic layer is visible, probably with waterproofing function. In some of the sections the organic layer was positive to Graaf test, thus showing the presence of animal glue. In most of the sections analysed we found an *imprimitura* layer containing lead white and lead-tin yellow (*giallolino*). Grinded glass is present in the *imprimitura* layer, recognizable by the presence of acute edged inclusion with a lower atomic weight, containing silicon, oxygen, sodium and calcium, probably with siccativ function [18–20] (see for example section 1131, Fig. 2b, layer B). Previous studies performed through not invasive molecular spectroscopic techniques, allowed the identification of an oil binder both in the *imprimitura* and in the paint layers, even it is not possible to exclude the possible addition of minor amounts of a protein component [13,14].

3.2. Cross-section 1131: original Raffaello layers and repaintings

One of the chosen sections for analytical insight is 1131, from the green dress of Grifonetto Baglioni, the young man holding up the dead Christ, in whose honor the painting was commissioned.² The section is very interesting, because it does contain different layers of green, including the heavy overpaintings (Fig. 2b, layers E, F; Fig. 1S in Supplementary Materials), which were no longer present in 2020, because removed in the intervention of 1966–72. SEM analysis highlighted over the *imprimitura* (layer B) the presence of different layers of green. From SEM-EDX, all the green layers are constituted by copper-based pigments, but some differences could be noted with reference to optical appearances in BSE images. Three very thin original layers³ containing defined copper-mineral particles are observable (C, D1, D2), carbon content in layers D1 and D2 is higher, thus suggesting the use of major amounts of oil binder to create semi-transparent glazes. In the upper two layers of repainting the copper distribution is diluted and the particles rich in this element are finely dispersed in the binder. This fine dispersion, the homogeneous distribution of copper and the absence of big, well-defined crystals brought to initial hypotheses on the composition of these two layers, suggesting the presence of copper resinate [19, 21], (Fig. 2c, layers E, F).

The presence of lead and tin in the original layers and in the first repainting one (layer E) also allowed to infer the presence of lead-tin yellow (*giallolino*) of the type I because no silicon, a characteristic element for the type II analogue, was detected [22]. These data add a new information to previous non-invasive analyses, where the diffuse presence of *giallolino* was detected through several technique, but no discrimination between the two types was inferred [3,7,13,14]. This pigment even allows us to state that the first not original layer it is an ancient repainting, dating back not later than mid-18th century, since lead-tin yellow was no longer used after then [19,22]. Second repainting layer F (more recent, instead) contains copper finely dispersed in the binder, lead and calcium.

Micro-Raman spectra obtained in two points of the green layer C above the white preparation (Fig. 2S in Supplementary Materials) evidenced a series of characteristic bands at 40, 59, 84, 114, 132, 154, 181, 198, 402, 435, 458, 768, 838, 1097 cm^{-1} . However, it is important to highlight some differences between the two spectra. In one of these (Fig. 2S, black line, point: R1), the peak at 402 cm^{-1} results remarkably higher in intensity, while a peak at 249 cm^{-1} results sharper; on the opposite, two signal at 269 and 292 cm^{-1} result strongly overlapping. In the other spectrum (Fig. 2S, grey line, R2), these last signals split in two defined peaks, while that one at 249 cm^{-1} broadens in a shoulder. The signal at 401 cm^{-1} is still evident, but decreases strongly in intensity, while the peak at 435 cm^{-1} results higher. Finally, a shoulder at 1062 cm^{-1} appears. The spectrum acquired in a point of layer above (Layer D1-D2, Fig. 3S, R3), shows a series of peaks at 42, 62, 83, 156, 182, 217 (shoulder), 273, 312, 359, 435, 515, 535, 571, 600, 721, 757, 984, 1061, 1098 cm^{-1} and, at higher wavenumbers, at 1307, 1367, 1493 and 1605 cm^{-1} . The hypothesis of a mixture of azurite and malachite arises from these data: if in the first point spectrum the high intensity of the signals at 249 and 402 cm^{-1} , along with the peaks at 84, 768 and 838 cm^{-1} , can be considered unambiguously identifier of the blue pigment, the signals at 154, 269 and 435 cm^{-1} , particularly evident in the second spectrum, can be attributed to malachite [23–26]. This is the dominant species in the third spectrum, where its presence is also confirmed by the signals at 1061, 1367, 1493 cm^{-1} . Moreover, according to the literature, some barely visible bands at 515 and 600 (very low intensity) cm^{-1} could be attributable to linarite, a mixed Pb and Cu hydroxy-sulphate, whose compresence with malachite is reported in literature [26], even if, in another paper, the signal at 515 cm^{-1} is assigned to malachite [23]. With reference to the association of azurite and malachite as minerals, it is not easy to assess if they were used in mixture or if one of the pigments is present as an impurity. However, further Raman mapping will be performed, in order to assess the distribution of the two species.

The Raman spectra acquired in the area of the first overpainting layer E (Fig. 4S, R4 and R7), present some signals at 81, 131, 197, 276, 293, 380, 460, 526 cm^{-1} , which are attributable to lead-tin yellow of type I [25,27]. The fingerprint features of the Raman

¹ Protein binder in the preparatory layer was identified already in the 1960s through the Graaf microchemical test performed on some of the sections.

² Atalanta Baglioni, mother of Federico Baglioni, known as Grifonetto, commissioned the young Raffaello Sanzio to paint the Deposition of Christ in order to glorify the memory of her dead son.

³ Upper portion of the third layer D2 contains a longitudinal fracture. It is not possible to establish whether the layer above D3 is part of D2 or a fourth pictorial layer applied by Raffaello.

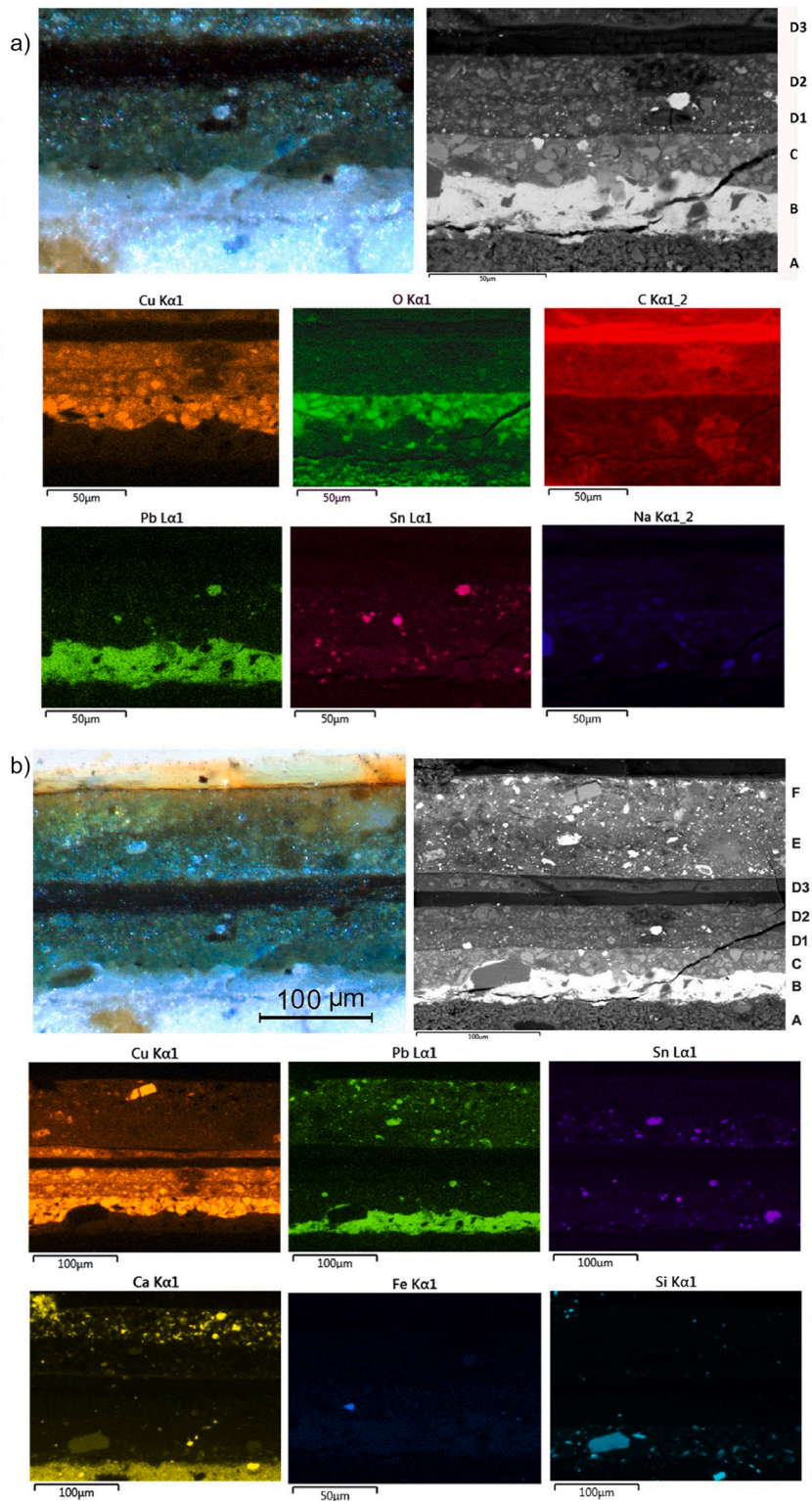


Fig. 2. Section 1131 (different areas): detail of original layers: optical microscope and SEM image (BSE), X-ray maps for copper, oxygen, carbon, lead, tin and sodium (a); Section 1131, original and overpainting layers, optical microscope and SEM image (BSE), X-ray maps for copper, lead, tin, calcium, iron, and silicon (b).

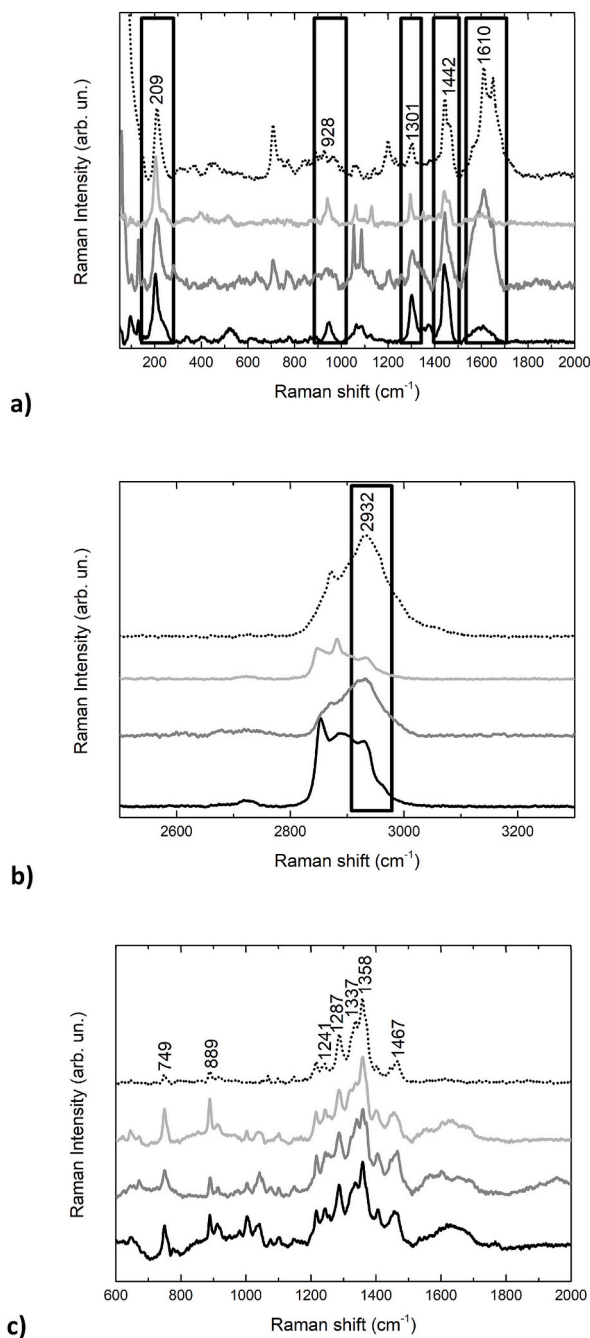


Fig. 3. Raman and SERS spectra of section 1131. Comparison of three spectra (solid lines) acquired in layers E and F with the spectrum of a standard of copper resinate (dot line) in the range 50–2000 cm^{-1} (a) and in the range 2500–3330 cm^{-1} (b), where typical bands of copper resinate are highlighted by the frame boxes; comparison of SERS spectra acquired for in layer E and F (solid lines) with the SERS spectrum of a standard of copper resinate (dot line) (c).

spectrum confirm the SEM-EDX elemental distribution and the consequent hypotheses: they allow achieving the discrimination between the possible two yellow pigments, which was not reached from the previous campaigns. Moreover, Raman allowed obtaining molecular information for the green pigments in the two green overpainting layers (E, F), where other three spectra were collected (Fig. 3; for further information on the location of the points, see Table 2S and Fig. 6S, R5, R6 and R11). In all these spectra, some signals were present around 209, 928, 1062, 1301, 1442, 1462 (shoulder), 1610, 2932 cm^{-1} , even if they could have slight variations in intensity and spectral shape in the different points. These peaks can be considered indicative of the copper resinate pigment, according to the literature [28–31]. It is worth to mention that the discrimination among verdigris, copper acetate and copper resinate

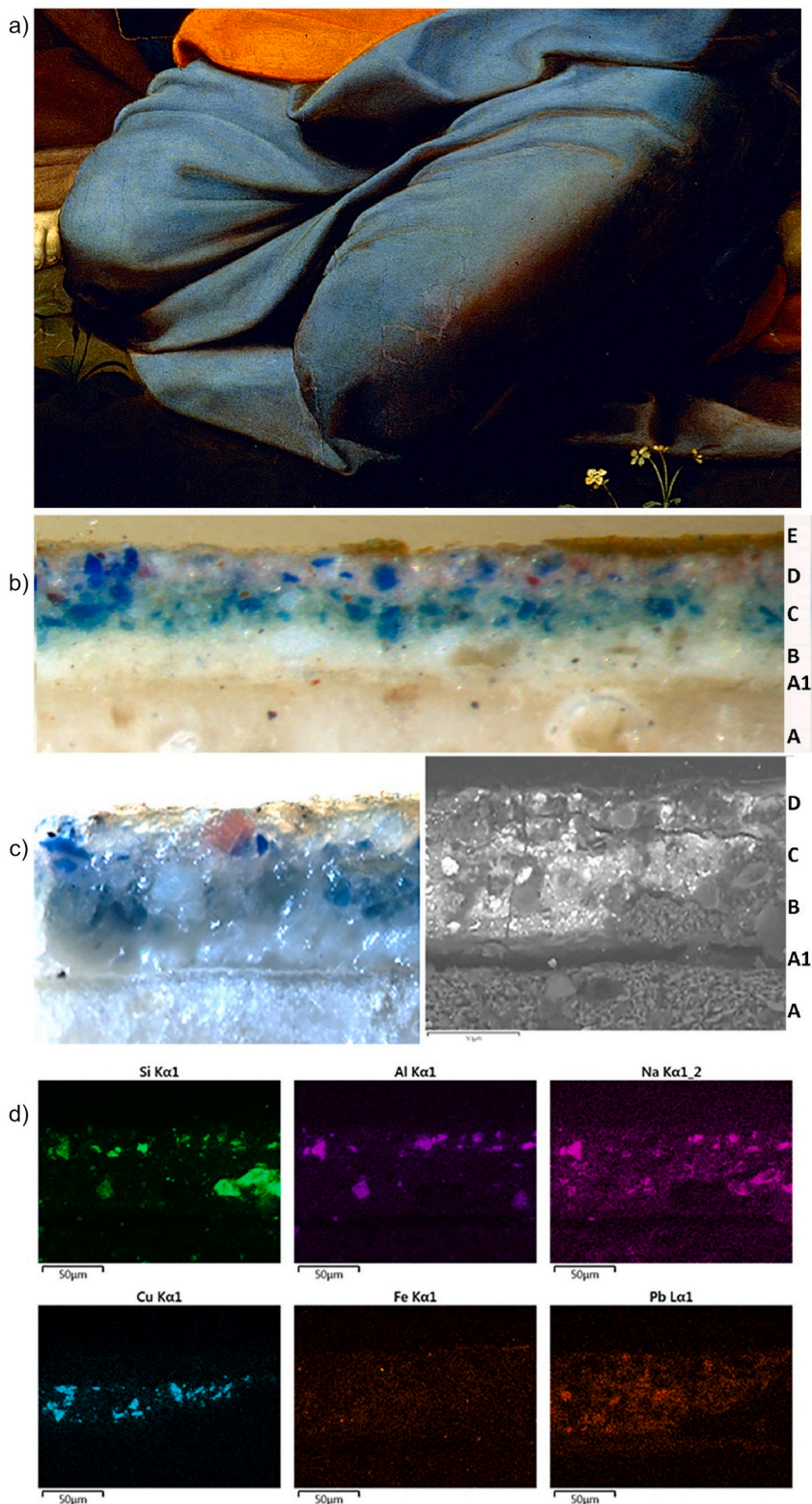


Fig. 4. Iridescent dress of the kneeling woman supporting the Virgin (a); optical microscope image of section 1522 (b); detail of section 1522, optical microscope and SEM image (BSE) (c); X-ray maps for silicon, aluminum, sodium, copper, iron and lead (d).

pigments is not ordinary, as pointed out in the mentioned studies. This ambiguity depends on both the manufacturing of the pigment (obtained dissolving verdigris and/or other copper salts with resinous materials [19,21]) and the ageing (where the processes of hydrolysis of resins and oils must be considered). However, in the case of analysed sample, the signals detected, along with the sets of bands generally attributable to organic material (in the ranges 1270–1700 and 2800–3050 cm^{-1}) suggest the use of the resinate species. This is also confirmed by the comparison with reference spectra of verdigris, copper acetate, copper basic acetate and copper resinate acquired with the same instrument: in Fig. 3a and 3b, the matching of the last spectrum with the general pattern of the sample spectra is remarkable, when no great correspondence could be observed with the other three (Fig. 6S). Only a signal at 707 cm^{-1} , observable merely in one of the sample spectra, would be attributable to verdigris according to the literature, but it is important to mention that this peak does not appear in the spectra of the laboratory references. Finally, the spectral pattern in the range of C–H

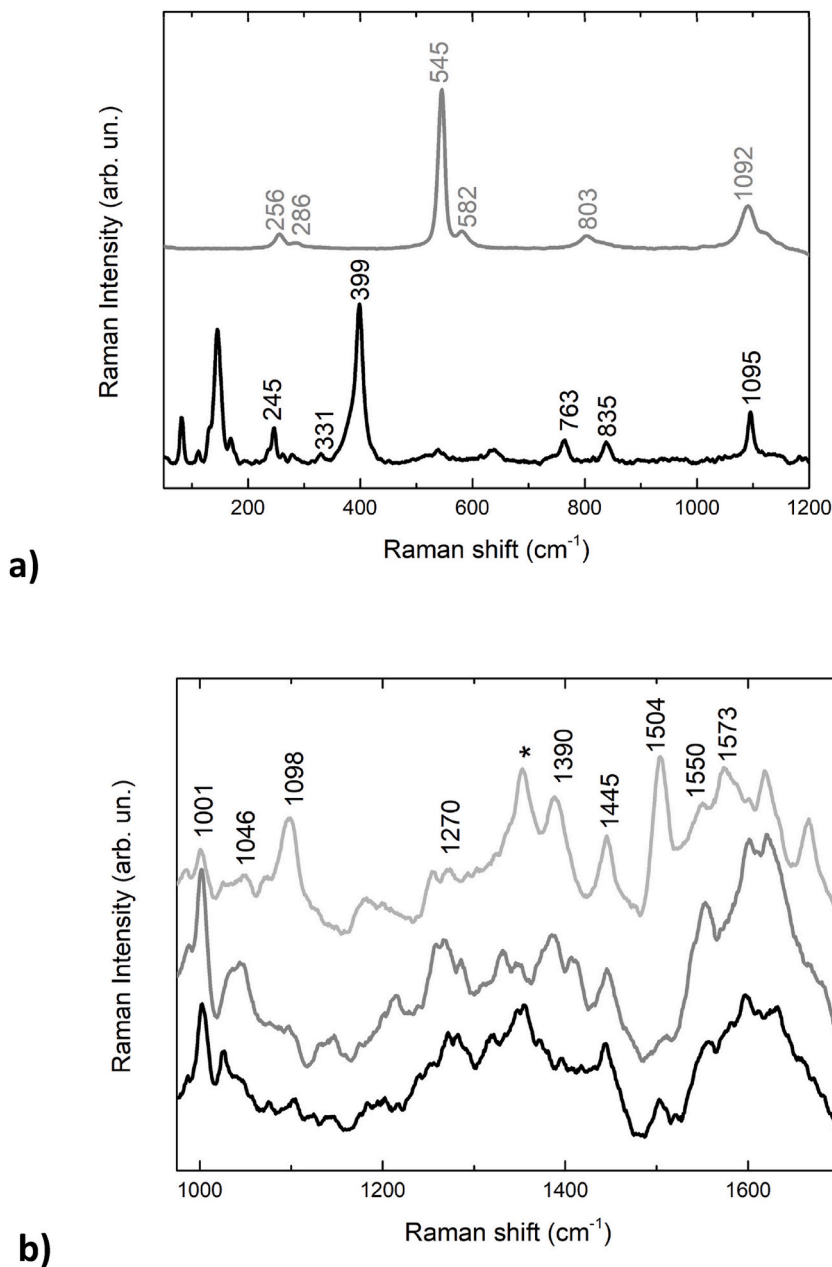


Fig. 5. Raman and SERS spectra from section 1522: comparison of a spectrum acquired in correspondence of a blue-green particle in layer C (black line, bottom), where the typical wavenumbers of azurite signals are highlighted, and a spectrum acquired in correspondence of a blue particle in layer D (grey line, top), where the typical wavenumbers of ultramarine signals are highlighted (a); comparison of SERS spectra obtained for one red particle in layer D, where the typical wavenumbers of insect-dye laje signals are highlighted, while the asterisk peak could present a contribution due to the colloidal paste (b).

stretching between 2800 and 3060 cm^{-1} , with intense signals varying from point to point, would suggest that, in the layers E and F, a species rich in different organic compounds is present, such as the resin components typical of a resinates. Two final spectra, acquired in an extended area in the green layer on the top F (Fig. 7S, R9 and R10), suggest the presence of a secondary copper compound in this surface layer: signals at 137, 197, 247, 321, 362, 391, 426, 448, 486, 596, 620, 964 and 1077 cm^{-1} are observable in these spectra and, from the comparison of the overall spectral pattern with the literature, the presence of posnjakite could be hypothesized [32]. Copper sulphates could have been present as impurities in the copper salt used to prepare copper resinates layer or could have been formed after degradation of copper resinates [33]. The Raman spectra, combined with morphological and elemental data from SEM-EDX, provided further insight. At first, it was possible to identify the molecular species constituting the green pigment in the Grifonetto's dress area, discriminating between a mixture of azurite and malachite for the original C, D1 and D2 layers, copper resinates on layer E and posnjakite -probably deriving from copper resinates, according to the morphological data-on layer F. This specific discrimination did not result from the published data, with the exceptions of some indirect hypotheses based on minor components: for instance, the compresence of barium and antimony impurities was addressed by Seccaroni [7] to the combination of blue and green pigments in this area, as confirmed by the Raman data here presented. The use of copper resinates, moreover, allows individuating a restoration intervention -dated before the mid-18th Century-older than those reported for the same area and dated after the first half of the 19th Century, for the presence of chrome and bismuth [7].

Finally, Raman analysis provided further information on the presence of extenders and white pigments in the overpainting layers. In one of the points, where copper resinates was found (Fig. 3 a, second spectrum from the bottom), the compresence of calcium carbonate would be suggested by relevant peaks at 154, 280, 707, 1086 cm^{-1} , while the high intensity of a peak at 1054 cm^{-1} would be attributable to the presence of lead white. Analogously, in a spectrum taken from the upper overpainting layer F (Fig. 5S, R8) a peak at 1086 cm^{-1} , along with a lower intensity peak at 713 cm^{-1} , would be indicative of calcium carbonate. This is confirmed by the spectrum collected in another point, where all the characteristic peaks of calcium carbonate are clearly visible (157, 283, 714, 1088 cm^{-1}) [24,25].

3.2.1. Cross-section 1131: SERS analyses

The presence of copper resinates, suggested by both SEM-EDX and supported by Raman spectroscopy, pushed the research towards new analytical strategies. With reference to the above-mentioned analytical issued in identifying this pigment and to its "hybrid" composition, the application of SERS spectroscopy for its recognition was tempted, which, according to our knowledge, represents a novel approach for this colouring species. Colloidal pastes were applied to the copper resinates standard, and SERS spectra were acquired (Fig. 3 c, dot line, SER1 and SER2). These presents high reproducibility and presents bands attributable to resinous materials

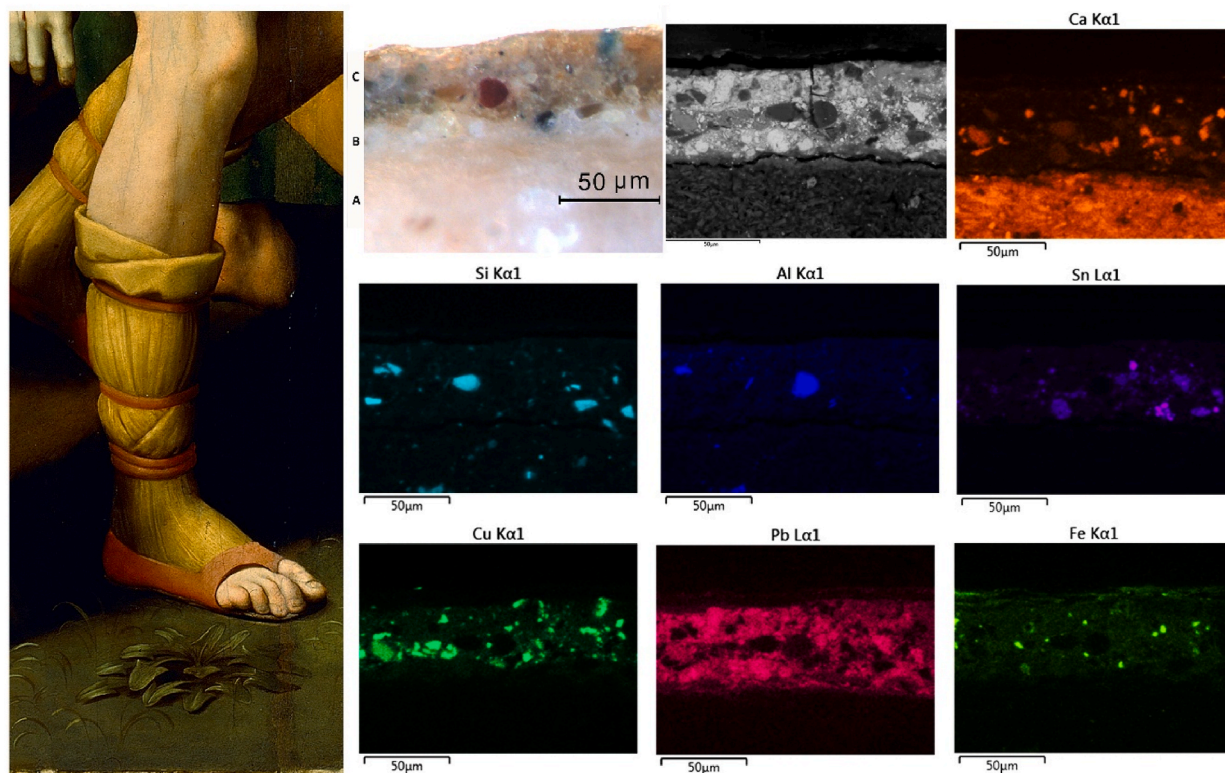


Fig. 6. Section 1517, area of sampling, optical microscope and SEM image (BSE), X-ray maps for calcium, silicon, aluminum, tin, copper, lead and iron.

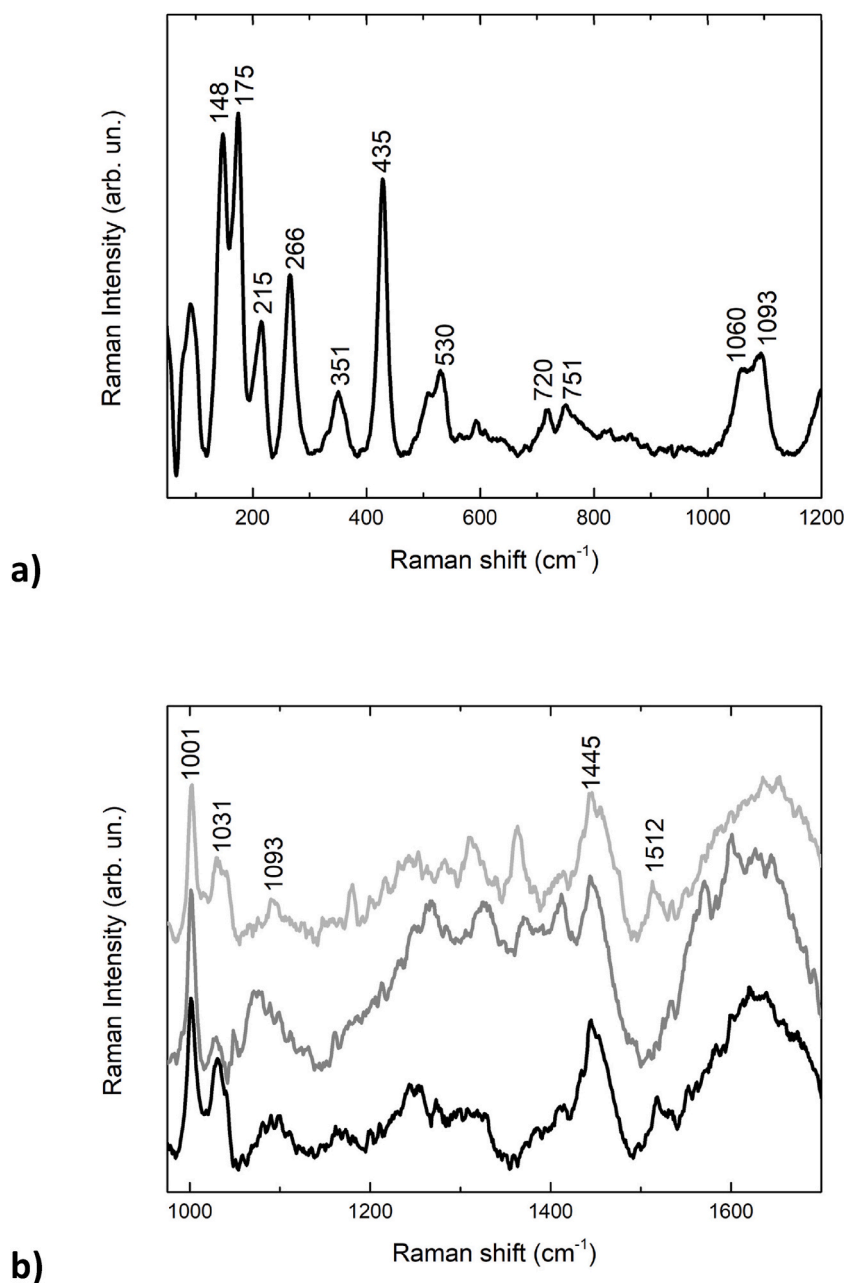


Fig. 7. Raman and SERS spectra from section 1517: Raman spectrum acquired on a green particle for the layer C, where the typical wavenumbers of malachite signals are highlighted (a); comparison of SERS spectra obtained for one red point in layer C (b).

and to copper resinate [28,34]. In particular, the recognizable peaks at 1287, 1338 and 1358 cm⁻¹, the first attributable to the twisting of CH₂ and the other two to CH₂ and CH₃ scissoring, along with lower intensity signals at 1403, 1446 and 1467 cm⁻¹. At lower wavenumbers, low intensity peaks at 749 and 889 cm⁻¹ are related to C–C ring stretching and CH₂ rocking, respectively. The signal at 1103 cm⁻¹ could be attributed to the C–C ring stretching, while the analogue at 1148 cm⁻¹ would be indicative of C–O–C asymmetric stretching. Peaks at 1216 and 1241 cm⁻¹ are attributed to CH=CH scissoring and C–O–H bending. It is interesting to notice that some bands could be considered SERS marker of copper resinate: for instance, the band at 1358 and 1467 cm⁻¹ result barely visible in standard Raman spectroscopy according to the literature, but they are clearly observable in the SERS spectra. This is furtherly confirmed by the spectra acquired on several points in the retouching layers in cross-section 1131 (Fig. 3 c, solid lines): these peaks are visible in all the reproducible spectra, while the general matching proves the presence of copper resinate, furtherly confirming SEM-EDX and Raman data.

3.3. Cross-section 1522

Cross section 1522 was sampled from the beautiful iridescent dress of the kneeling woman supporting the Virgin. In the cross section it is possible to distinguish the gypsum preparatory layer A, an organic waterproofing layer A1, the whitish *imprimitura* B, and two different layers of blue: the first with a greenish tone (C) and the second (D) containing blue and red particles (Fig. 4a). SEM-EDX analyses evidenced granules of lead and of copper in the first blue layer C, suggesting the use of azurite and lead white, while the second blue layer D contains lead, silicon, aluminum, sodium, elements attributable to lead white and ultramarine blue (Fig. 4b, c, d). Some of the red particles in the upper layer D, as that shown in Fig. 4c, with a rounded appearance and a more transparent shade than other red granules, contain aluminum and sulfur, letting to suppose the use of a red lake adsorbed on alum [35]. On the upper portion of the section it is possible to recognize the discontinuous organic layer of browned varnish (E).

Raman spectra acquired from section 1522 in correspondence of blue-green particles of the first pictorial layer above the preparation (C), show the typical signals of azurite at 112, 131 (shoulder), 139, 172, 177, 194, 237, 245, 331, 399, 763, 835, 1095 cm^{-1} [23–26] (Fig. 5 a, black line; Fig. 8S, R1, R2 and R3). Some signals show variable intensities in the different spectra: for instance, a peak at 1053 cm^{-1} is observable in only two points and likely attributable to lead white [24,25,36], along with a very weak signal at around 680 cm^{-1} , while, in one of the spectra, a very strong peak at 145 cm^{-1} could be indicative of the presence of massicot or litharge [24, 25,27,36]. The spectrum acquired on a brown-reddish particle on the layer C is quite complex for the interpretation: in this spectrum (Fig. 9S, R7), if the peaks at 81, 136 and 282 (broad band) cm^{-1} would be indicative of lead-tin yellow of type I, three bands at 395, 565 (shoulder) and 680 cm^{-1} are not assignable to this species. If the band at 395 cm^{-1} could be considered indicative of goethite (a component of yellow ochre) [37,38], the same band, along with the other two, it could be attributed also to the presence of celadonite, a component of green earth pigments [39]. These species would be minor components of the film.

On the purplish-blue layer D, above the blue-green layer C, two Raman spectra were collected on blue particles (Fig. 5 a, grey line; Fig. 10S, R4 and R6); these are characterized by signals at 256, 286, 545, 582, 803, 831 (shoulder), 1091 and 1120 (shoulder) cm^{-1} . This set of signals is attributable to the use of ultramarine blue [24,25,40,41]. Moreover, in the same layer some red particles appear. In the spectrum acquired in correspondence of one among these, the typical peaks of red ochre at 224, 291, 410, 497, 613, 662 cm^{-1} , where the first five peaks are attributable to hematite and the last one to maghemite [37,38] (Fig. 11S, R5 and R9). The signals of red ochre also appear, even if in a lower quality spectrum, in correspondence of another reddish particle in the same layer, while, the spectrum collected for a brownish particle in layer C (Fig. 12S, R8), show peaks at 87, 243, 297, 387, 481, 577 (broad band), 679 cm^{-1} , these are attributable to goethite [37,38].

These data result quite important, because the pigments of the iridescent blue drapery of the woman on the Virgin knees have never been fully characterized. The identification of azurite confirms the XRF data reported in literature, which highlighted the presence of copper [3,4,7]. No specific mention to ultramarine blue in this area was published with reference to XRF measurements [3,7], except for the detected silicon and potassium, which, however, could be related to other species, since their ubiquitous distributions in several pigments. The presence of a layer of ultramarine on azurite results coherent with both Raffaello and the other contemporary Italian masters [42], and it was identified by Miliani et al. [13,14] in the *Deposition* through Reflectance mid-InfraRed spectroscopy, but not for this iridescent area. An interesting aspect resulting from the Raman spectra is represented by minor compounds present in C and D layers. For instance, the presence of lead-tin yellow of type I is reported not only in the *imprimitura*, along other lead-based pigments in the C layer. In the D one, instead, both lead- and iron-based pigments are present as single particles: this confirms the XRF elemental data [3,7], adding information on their specific nature and on their distribution in the layers (not achievable directly through the non-invasive techniques). It is also interesting to highlight that no cinnabar was observed through Raman spectroscopy, in agreement with the XRF data but in contrast with FORS results published by Miliani [13,14]. Considering of the presence of different pigments in fine particles in these layers, it is possible to hypothesize that cinnabar is present as well as a minor component, and its distribution could vary from point to point in the same area. However, the richness of several reddish and brown pigments could be in charge for the brilliant iridescence of the drapery.

Finally, an interesting aspect to deepen is related to the presence of lake pigments. According to the previously published data, lakes should be present in several red, purple and pink areas and they are frequently associated to a remarkable manganese content in the painting, which would correspond to powder glass added to the lake. However, in the area corresponding to the iridescent drapery, no manganese was identified by Seccaroni et al. [3,7], while Miliani [13,14] reports the presence of manganese. Taking into account of these differences, likely due to the punctual presence of red particles, the identification of red lakes on this cross-section was tempted through SERS spectroscopy.

3.3.1. Cross-section 1522: SERS analyses

Some spectra were acquired on different points of the purplish blue layer D, where red particles not containing iron were present, in correspondence of silver clusters deriving from the colloidal paste. The SERS spectra obtained did not present a high reproducibility (Fig. 5 b, SER1), but some features resulted observable in most the spectra, with variations in the relative intensity, such as signals around 750, 1001, 1046, 1098, 1138, 1202, 1265–1270, 1353 (possible overlapping with a colloidal paste peak), 1376–1388, 1410, 1445, 1504, 1550, 1608, 1620 cm^{-1} . Moreover, in some points some further peaks appear at 1125, 1135–1146, 1181, 1202–1213, 1291–1302, 1325–1336, 1526 cm^{-1} . From these data, it is possible to find some similarities with the SERS bands of anthraquinone-based dyes: the band at 1291 cm^{-1} would be indicative of C–OH bending, the signal at 1388 cm^{-1} of ring C–C stretching, the band at 1577 cm^{-1} is likely indicative of ring C–C stretching modes, while, finally, the shoulder at 1608 cm^{-1} is attributed to a combination of C–C bonds and C=O interaction with Ag nanoparticles [43]. The precise assignation of the specific dye is not easy, because some differences with the SERS spectra of specific chromophores are observable. However, through reference with some studies, it is

possible to find a certain correspondence with the typical signals of anthraquinone-based signals from insect sources. In particular, signals at 1146, 1336, 1376, 1445, 1550 and 1608 cm^{-1} could be attributed to the use of kermes lake or to lac dye [43–46], even if the high presence in all the spectra of the signal at 1445, along with some minor features at 1046 and 1098 cm^{-1} would suggest for the second. However, it is important to highlight that these peaks would have also a minor correspondence with the SERS spectra reported in literature for some madder lakes [16,47].

3.4. Cross-section 1517

The last section analysed is 1517, coming from the dull green of the ground, a green obtained by mixing many pigments. SEM analyses showed that pictorial layer C over the *imprimitura* B, about 50 μm thick, contains copper, iron, silicon, potassium, lead and tin, attributable to a mixture of malachite, lead white, lead-tin yellow, and a mixture of earths and/or others (Fig. 6).

Micro-Raman with 632.8 laser excitation completed and confirmed SEM-EDX data. The spectrum acquired on a green particle (Figs. 7 and 13S, R1) is characterized by signals at 90, 148, 176, 216, 264, 351, 427, 509 (shoulder), 530, 598, 719, 748, 1067 (shoulder) and 1096 cm^{-1} . This set of signals, as highlighted for the cross-section 1131, is attributable to the presence of malachite. The spectrum acquired on a red-orange particle presents a low signal/noise ratio, but it is possible to distinguish a high intensity band at 388 cm^{-1} , along with lower intensity signals at 86, 247, 297, 553, 676 cm^{-1} , these last two as broad bands, (Fig. 14S, R2). With reference to the literature, these signals can be attributed to a material rich in goethite, as a yellow ochre [37,38]. The spectrum acquired on the top layer, presents only two signals at 91 and 141 cm^{-1} , with a barely visible peak at 289 cm^{-1} and a broader band around 625 cm^{-1} (Fig. 15S, R3). The three first signals are attributable to the presence of litharge [24,25,27,36].

These data generally confirm the information obtained from XRF, providing new insights into the specific molecule identification. The use of malachite for the ground is complementary to the hypothesis of verdigris/copper resinate for the trees by Seccaroni [3], while the pigments used to obtain a duller color are the yellow ochre and the litharge. This confirms the MA-XRF data, which highlighted the presence of iron and lead in this area [7]. Similarly to section 1522, also in section 1517, rounded red particles are visible in which the SEM analysis highlights aluminum and sulfur, probably attributable to red lake. These species could have been added in order to give a particular shade to the ground. Further analyses were performed through SERS spectroscopy, addressed to investigate the lake pigments, in order to fulfill the complete characterization of the present materials.

3.4.1. Cross-section 1517: SERS analyses

The SERS spectra acquired for one of the Al-rich particle (Fig. 7 b, SER1) are quite reproducible in the overall pattern, even if the signal/noise ratio is not high. In all of them, signals at 1001, 1031, 1260, 1317, 1370, 1445, 1518 and 1600 cm^{-1} are observable. This pattern presents a certain similarity with the spectra obtained for cross-section 1522 and it confirms a general correspondence with the SERS spectra of lac and kermes dyes [43–46], supporting the hypothesis of one of these two dyes formulated also for the cross-section 1522. The distinction between these two insect dyes it is not easy, because the major chromophores present similar structures and, in general, insect dyes present lower affinity for metal nanoparticles than plant-based ones (e.g. madder) for reasons related to chromophore structures, pH and nanoparticle charges [44,46]. The high intensity for the band at 1445 cm^{-1} in cross-section 1517 would suggest the lake is based on lac dye, as well as the presence of signals at 1001–1003 cm^{-1} and at 1031–1045 cm^{-1} . However, it is fundamental to mention these last bands -considered specific markers of laccaic acids [46]- are characterized by some differences in Raman shift in comparison to the literature, while their general pattern does not correspond in relative intensity to what reported and expected for lac dye SERS spectra. In general, the overall quality of the spectra and some ambiguities with the literature cannot allow excluding the use of kermes or other insect lakes.

With reference to data obtained for this cross-section and the 1522, it is important to highlight that, between 1966 and 1972, no samples for stratigraphic sections were taken from red areas. Rare red granules, which could be analysed, are present only in the investigated sections of the ICR archive. The non-invasive elemental investigations performed so far on the *Deposition* [1–4,7,8] have made it possible to recognize the use of cinnabar in the red backgrounds, such as the robe of Grifonetto, the shoes of Grifonetto and of the transporter on the left, the robe of the kneeling woman, while small quantities of cinnabar were used to modulate the color of hair or skin tones. Other red areas such as the cloak of Saint John or the shirt of Magdalene were made only with red lake, while glazes of lakes over the cinnabar cannot be fully identified. Not invasive molecular investigation on red areas [13,14] have allowed to identify the presence of a kermes lake. Our SERS results could be considered in general agreement with those deriving from previous non-invasive campaigns, while these colouring materials are reported in Raffaello's production [9–12]. Even if the study of a cross section from a red area from the *Deposition* would have brought very interesting results, new sampling has been chosen to be avoided for ethical reasons, as mentioned before. Nonetheless, further measurements appear to be necessary for the purpose of unique determination of the specific insect dye, which demands for novel approaches [48–50].

4. Conclusions

The *Deposition* is so far one of the most studied painting by means of not invasive techniques. These allowed the characterization of most of the pigment present in the palette and of the oil as a binder [1–14].

The study we presented allowed to obtain additional information to the knowledge of Raffaello's painting technique, since the combination of elemental and molecular analysis on the cross sections allowed to determine the precise location in the stratigraphy of pigments and also to solve some ambiguities not fully solved in previous campaigns. The study conducted on the selected cross section from the *Deposition*, by the combined use of SEM-EDX, micro-Raman and SERS with 632.8 nm laser excitation, has made it possible to

complete the reading of the stratigraphies and to obtain more in-depth and specific information about the materials present in the preparatory and in each pictorial layer. The combination of elementary and molecular micro-analysis techniques, performed on the same pigment granules within the pictorial layers of three different stratigraphic sections, has made it possible to recognize the chemical composition of the pigments present, even if in trace amounts.

In general, investigations have shown that the paint layers are not made up of simple pigments, but each gradation is obtained by mixing different pigments, some sometimes in very small quantities. Skillful and fine brushstrokes are characteristic of Raffaello's technique. The color tone was calibrated very precisely on the palette, by combination of many different pigments in small quantities to obtain the desired nuance. Often the color gradations are obtained with very thin different superimposed layers.

Several inorganic species were detected and identified by means of the two techniques, which resulted robustly complementary and allowed reconstructing the palette and the technique used by the artist for the analysed painting. With reference to the previously published results obtained by non-invasive techniques, molecular analysis allowed to determine that lead white was not the only lead containing pigment, but also lead oxides were present. In this perspective, several interesting data involve the detection of lead-tin yellow. It has to be mentioned that the presence of lead-tin yellow was evidenced though not invasive techniques [7,13,14]. However, it was not possible to determine: 1) in which layer the pigment was employed; 2) if lead-tin yellow of type I was employed. The combination of elemental and molecular investigation on the cross sections allowed to determine that the type I-pigment is present in both the *imprimatura* layer and in the green and greenish paint layers, with reference the absence of silicon in the grains specifically distributed in the above-mentioned layers and the fingerprint pattern of the Raman spectra.

An interesting aspect is related to the specific identification of copper-based green pigments, which represent a traditional problem in paintings diagnostics. While the original 1972 report from ICR did not include any experimental data, non-invasive campaigns only identified the presence of copper in several green area. In the present study, a combination of malachite and azurite, along with lead-tin yellow of type I and lead white, is assessed in Grifonetto's dress, while malachite is used for the ground, mixed with litharge and yellow ochre. Copper resinate -hypothesized in the 1972 study [4], without however being able to state precisely where, and by Seccaroni in 2010 only for the trees [3], were not found in the original layers of cross-section, but only in the two repainting ones on Grifonetto's cloth. Taking into account of the stratigraphy of other cross-sections, these findings can be extended to the repainted green areas of section 1565, 1566, 1634, 1916 (Table 1S). Interestingly, from the point of view of the conservative history of the masterpiece, the presence of copper resinate in the two repainting layers, along with lead-tin yellow of type I, made it possible to classify them chronologically: the first layer dates not later than mid-18th century, the second on the top is more recent. These interventions occurred before a third intervention after 1850s, individuated with reference to previous XRF data [3,7]. In this perspective, the SEM morphological and elemental analysis suggested the preliminary hypothesis of the presence of resinate pigment, which was confirmed by Raman spectroscopy through molecular fingerprint. The combination of the techniques resulted in the identification of this species, whose discrimination is not easy from an analytical point of view. However, with reference to the variability of the signals of copper resinate due to its complex composition, further efforts were addressed to test SERS analysis for the identification of this typology of pigment. Surprisingly, the SERS spectra obtained for both the reference and the analysed area in section 1131 presented high reproducibility and a remarkable matching. This method shows a great potential for the identification of this species, and it should be implemented with further research— for instance, SERS spectra for several copper resinates, obtained by means of different recipes, should be acquired and compared. According to our best knowledge, this represents the first reported identification of copper resinate through SERS analysis.

With reference to the previous studies devoted to the identification of organic lake pigments [13,14], SERS analyses were also performed on the cross-sections 1522 and 1517, in correspondence of red particles. The presence of an anthraquinone lake was suggested, and, in particular, a lake based on kermes or on laccaic acids should represent the most probable one. However, the use of colloidal pastes on these samples must be adjusted, in order to improve the reproducibility of the analyses, especially for the identification of insect-based lakes, which present lower affinity for nanoparticles, also according to the literature [44]. With reference to these issues in the identification of these organic-based pigments -such as copper resinate and anthraquinone lakes-further research, based on the use on more advanced approaches of vibrational spectroscopies (e.g. synchrotron radiation probe), is actually under study in order to deepen the investigation through a novel integrated protocol.

Finally, this study represents an interesting proof of concept in the application of newer methodologies to old cross-sections, which has the potential of extending the amount of information available from historical archives through sustainable and affordable approaches from the point of view of conservation and diagnostic.

This research did not receive any specific grant from funding agencies in the public, commercial, or not-for-profit sectors.

Data availability statement

No data have actually been deposited into a publicly available repository.

CRedit authorship contribution statement

Marcella Ioele: Writing – original draft, Investigation, Conceptualization. **Alessandro Ciccola:** Writing – original draft, Investigation, Data curation. **Paolo Postorino:** Supervision.

Declaration of competing interest

The authors declare that they have no known competing financial interests or personal relationships that could have appeared to influence the work reported in this paper.

Acknowledgements

The authors thank Drs. Marisa Laurenzi Tabasso, Natalia Macro, Giulia Germinario, Greta Peruzzi, Ilaria Serafini and Biagio Valenti for their contribution to the realization of this study. The Open Access publication of the paper was funded by Sapienza, in the frame of Award Horizon Europe 2022 project (Coordinator: Prof. Gabriele Favero).

Appendix A. Supplementary data

Supplementary data to this article can be found online at <https://doi.org/10.1016/j.heliyon.2024.e35597>.

References

- [1] M. Minozzi, Raffaello nella Galleria Borghese. Nuove indagini e un progetto di conservazione programmata, Cinisello Balsamo (MI), Silvana Editoriale, 2023. ISBN: 88-366-4605-0.
- [2] R. Alberti, T. Frizzi, M. Gironda, M. Occhipinti, T. Parsani, C. Seccaroni, A. Tatì, From noise to information. Analysing macro.XRF mapping of strontium impurities in Raphael's Baglioni Entombment in the Galleria Borghese, Rome, *J. Cult. Herit.* 58 (2022) pp130–136.
- [3] P. Moioli, C. Seccaroni Il progresso dell'analisi di fluorescenza X nello studio della tecnica pittorica: imprimitura, caratterizzazione e qualità dei pigmenti. La Deposizione Baglioni, in: K. Hermann-Fiore (Ed.), Raffaello: la Deposizione in Galleria Borghese, il restauro e studi storico-artistici, Federico Motta, 2010, pp. 206–2013. ISBN:88-7179-581-4.
- [4] L. Ferrara, S. Staccioli, A.M. Tantillo, Storia e restauro della Deposizione di Raffaello. Museo e Galleria Borghese, Roma, 1972.
- [5] M. Ioele, M. Laurenzi Tabasso, Analisi delle sezioni stratigrafiche "storiche" conservate presso l'archivio ICR, in: M. Minozzi (Ed.), Raffaello nella Galleria Borghese. Nuove indagini e un progetto di conservazione programmata, Cinisello Balsamo (MI), Silvana Editoriale, 2023, pp. 150–163. ISBN: 88-366-4605-0.
- [6] M. Ioele, A. Ciccola, P. Postorino, Deposition by Raffaello Sanzio, analytical insights on cross sections for the characterisation of pictorial palettes, in: TECHNART 2023 LISBON | 07/12 MAY Int. Conf. Anal. Tech. Art Cult. Heritage; B. Abstr., n.d. <https://doi.org/10.34619/ipq7-vuaj>.
- [7] R. Alberti, C. Bertorello, T. Frizzi, M. Gironda, M. Occhipinti, T. Parsani, C. Seccaroni, La Deposizione Baglioni: studio dei materiali attraverso le mappe di concentrazione degli elementi ottenute con la tecnica MA.XRF, in: M. Minozzi (Ed.), Raffaello nella Galleria Borghese. Nuove indagini e un progetto di conservazione programmata, Cinisello Balsamo (MI), Silvana Editoriale, 2023, pp. 108–117. ISBN: 88-366-4605-0.
- [8] C. Maltese, S. Sciuti, Resoconto sommario di analisi sematometriche e chimico fisiche non distruttive eseguite su quattro dipinti di Raffaello e la sua cerchia, in: Raffaello Nelle Raccolte Borghese, Catalogo Della Mostra (Roma, Galleria Borghese Gennaio-Marzo 1984), Roma, 1984.
- [9] A. Roy, M. Spring, The Deposizione Baglioni (1507), in Raphael's painting technique: working practices before Roma. Proceedings Eu-Artex Workshop, (London, National Gallery, 11 nov 2004), Firenze, 2007, pp. 109–114.
- [10] A. Roy, M. Spring, C. Plazzotta, Raphael's early work in the national Gallery : paintings before Rome linked r, *Natl. Gall. Tech. Bull.* 25 (2004) 4–35.
- [11] K. Hermann-Fiore, Raffaello: la Deposizione in Galleria Borghese, il restauro e studi storico-artistici, Federico Motta, 2010. ISBN:88-7179-581-4.
- [12] A. Cerasuolo, A. Zezza, Raffaello a Capodimonte, L'officina dell'artista, Editori Paparo, 2021.
- [13] C. Miliani, C. Ricci, F. Rosi, A. Sassolini, F. Presciutti, C. Clementi, A. Romani, B. Brunetti, A. Sgamellotti, C. Seccaroni, P. Moioli, The deposizione Baglioni (1507), non-invasive study of raphael's palette by complementary molecular spectroscopic techniques from X-rays to the near infrared. Conference: Proceedings of the Workshop "Raphael Painting Technique: Working Practice before Rome", Volume: Quaderni di Kermes 107-112), NARDINI PRESS S.R.L., 2007. ISBN-10 8840442928.
- [14] B.G. Brunetti, C. Clementi, C. Miliani, C. Ricci, A. Romani, F. Rosi, A. Sgamellotti, Studio della tecnica pittorica della Deposizione tramite analisi spettroscopiche molecolari non invasive, in: K. Hermann-Fiore (Ed.), Raffaello: la Deposizione in Galleria Borghese, il restauro e studi storico-artistici, Federico Motta, 2010, pp. 199–201. ISBN:88-7179-581-4.
- [15] G. Sidoti, F. Talarico, M.G. Vigliano, I materiali e la tecnica esecutiva di Caravaggio attraverso lo studio delle sezioni stratigrafiche "storiche", *Boll. ICR.* (2011) 55–75.
- [16] A. Idone, M. Aceto, E. Diana, L. Appolonia, M. Gulmini, Surface-enhanced Raman scattering for the analysis of red lake pigments in painting layers mounted in cross sections, *J. Raman Spectrosc.* 45 (2014) 1127–1132, <https://doi.org/10.1002/jrs.4491>.
- [17] N. Leopold, B. Lendl, A new method for fast preparation of highly surface-enhanced Raman scattering (SERS) active silver colloids at room temperature by reduction of silver nitrate with hydroxylamine hydrochloride, *J. Phys. Chem. B* 107 (2003) 5723–5727, <https://doi.org/10.1021/jp027460u>.
- [18] K. Lutzenberger, H. Stege, C. Tilenschi, A note on glass and silica in oil paintings from the 15th to the 17th century, *J. Cult. Herit.* 11 (2010) 365–372, <https://doi.org/10.1016/j.culher.2010.04.003>.
- [19] R.L. Feller, A. Roy, Artists' pigments: a handbook of their history and characteristics, Volume 2, National Gallery o.
- [20] E. Manzano, R. Blanc, J.D. Martin-Ramos, G. Chiari, P. Sarrazin, J.L. Vilchez, A combination of invasive and non-invasive techniques for the study of the palette and painting structure of a copy of Raphael's Transfiguration of Christ, *Herit. Sci.* 9 (2021) 150, <https://doi.org/10.1186/s40494-021-00623-z>.
- [21] R. Woudhuyzen-Keller, Aspects of painting technique in the use of verdigris and copper resinates, in: A. Wallert, E. Ermens, M. Peek (Eds.), *Hist. Paint. Tech. Mater. Stud. Pract. Prepr. A Symp. Univ. Leiden, Netherlands, the J. Paul Getty Trust*, 1995, pp. 65–69.
- [22] R. Šefců, S. Chlumská, A. Hostašová, An investigation of the lead tin yellows type I and II and their use in Bohemian panel paintings from the Gothic period, *Herit. Sci.* 3 (2015), <https://doi.org/10.1186/s40494-015-0045-2>.
- [23] R.L. Frost, W.N. Martens, L. Rintoul, E. Mahmutagic, J.T. Klopogge, Raman spectroscopic study of azurite and malachite at 298 and 77 K, *J. Raman Spectrosc.* 33 (2002) 252–259, <https://doi.org/10.1002/jrs.848>.
- [24] I.M. Bell, R.J.H. Clark, P.J. Gibbs, Raman spectroscopic library of natural and synthetic pigments (pre- approximately 1850 AD), *Spectrochim. Acta. A. Mol. Biomol. Spectrosc.* 53A (1997) 2159–2179, [https://doi.org/10.1016/S1386-1425\(97\)00140-6](https://doi.org/10.1016/S1386-1425(97)00140-6).
- [25] L. Burgio, R.J.H. Clark, Library of FT-Raman spectra of pigments, minerals, pigment media and varnishes, and supplement to existing library of Raman spectra of pigments with visible excitation, *Spectrochim. Acta. A. Mol. Biomol. Spectrosc.* 57 (2001) 1491–1521, [https://doi.org/10.1016/S1386-1425\(00\)00495-9](https://doi.org/10.1016/S1386-1425(00)00495-9).
- [26] M. Bouchard, D.C. Smith, Catalogue of 45 reference Raman spectra of minerals concerning research in art history or archaeology, especially on corroded metals and coloured glass, *Spectrochim. Acta Part A Mol. Biomol. Spectrosc.* 59 (2003) 2247–2266, [https://doi.org/10.1016/S1386-1425\(03\)00069-6](https://doi.org/10.1016/S1386-1425(03)00069-6).

- [27] R.J.H. Clark, L. Cridland, B.M. Kariuki, K.D.M. Harris, R. Withnall, Synthesis, structural characterisation and Raman spectroscopy of the inorganic pigments lead tin yellow types I and II and lead antimonate yellow: their identification on medieval paintings and manuscripts, *J. Chem. Soc. Dalton Trans.* (1995) 2577–2582, <https://doi.org/10.1039/DT9950002577>.
- [28] C. Conti, J. Striova, I. Aliatis, E. Possenti, G. Massonnet, C. Muehlethaler, T. Poli, M. Positano, The detection of copper resinate pigment in works of art: contribution from Raman spectroscopy, *J. Raman Spectrosc.* 45 (2014) 1186–1196, <https://doi.org/10.1002/jrs.4455>.
- [29] J. Buse, V. Otero, M.J. Melo, New insights into synthetic copper greens: the search for specific signatures by Raman and infrared spectroscopy for their characterization in medieval artworks, *Heritage* 2 (2019) 1614–1629, <https://doi.org/10.3390/heritage2020099>.
- [30] L.B. Brostoff, C. Connelly Ryan, Tracing the alteration of verdigris pigment through combined Raman spectroscopy and X-ray diffraction, part i, *Restaurator* 41 (2020) 3–30, <https://doi.org/10.1515/res-2019-0007>.
- [31] M. San Andrés, J.M. De La Roja, V.G. Baonza, N. Sancho, Verdigris pigment: a mixture of compounds. Input from Raman spectroscopy, *J. Raman Spectrosc.* 41 (2010) 1178–1186, <https://doi.org/10.1002/jrs.2786>.
- [32] R.L. Frost, Raman spectroscopy of selected copper minerals of significance in corrosion, *Spectrochim. Acta Part A Mol. Biomol. Spectrosc.* 59 (2003) 1195–1204, [https://doi.org/10.1016/S1386-1425\(02\)00315-3](https://doi.org/10.1016/S1386-1425(02)00315-3).
- [33] S. Švarcová, D. Hradil, J. Hradilová, E. Kočí, P. Bezdička, Micro-analytical evidence of origin and degradation of copper pigments found in Bohemian Gothic murals, *Anal. Bioanal. Chem.* 395 (2009) 2037–2050, <https://doi.org/10.1007/s00216-009-3144-7>.
- [34] D. Lau, M. Livett, S. Praver, Application of surface-enhanced Raman spectroscopy (SERS) to the analysis of natural resins in artworks, *J. Raman Spectrosc.* 39 (2008) 545–552, <https://doi.org/10.1002/jrs.1878>.
- [35] Jo Kirby, Marika Spring, Catherine Higgitt, The technology of red lake pigment manufacture: study of the dyestuff substrate, *National Gallert Technical Bulletin* 26 (2005) 71–87.
- [36] L. Burgio, R.J.H. Clark, S. Firth, Raman spectroscopy as a means for the identification of plattnerite (PbO₂), of lead pigments and of their degradation products, *Analyst* 126 (2001) 222–227, <https://doi.org/10.1039/b008302j>.
- [37] M. Hanesch, Raman spectroscopy of iron oxides and (oxy)hydroxides at low laser power and possible applications in environmental magnetic studies, *Geophys. J. Int.* 177 (2009) 941–948, <https://doi.org/10.1111/j.1365-246X.2009.04122.x>.
- [38] D.L.A. de Faria, S. Venâncio Silva, M.T. de Oliveira, Raman microspectroscopy of some iron oxides and oxyhydroxides, *J. Raman Spectrosc.* 28 (1997) 873–878, [https://doi.org/10.1002/\(SICI\)1097-4555\(199711\)28:11<873::AID-JRS177>3.0.CO;2-B](https://doi.org/10.1002/(SICI)1097-4555(199711)28:11<873::AID-JRS177>3.0.CO;2-B).
- [39] F. Ospitali, D. Bersani, G. Di Lonardo, P.P. Lottici, 'Green earths': vibrational and elemental characterization of glauconites, celadonites and historical pigments, *J. Raman Spectrosc.* 39 (2008) 1066–1073, <https://doi.org/10.1002/jrs>.
- [40] R.J.H. Clark, M.L. Franks, The resonance Raman spectrum of ultramarine blue, *Chem. Phys. Lett.* 34 (1975) 69–72, [https://doi.org/10.1016/0009-2614\(75\)80202-8](https://doi.org/10.1016/0009-2614(75)80202-8).
- [41] I. Osticioli, N.F.C. Mendes, A. Nevin, F.P.S.C. Gil, M. Becucci, E. Castellucci, Analysis of natural and artificial ultramarine blue pigments using laser induced breakdown and pulsed Raman spectroscopy, statistical analysis and light microscopy, *Spectrochim. Acta Part A Mol. Biomol. Spectrosc.* 73 (2009) 525–531, <https://doi.org/10.1016/j.saa.2008.11.028>.
- [42] J.D. Martín-Ramos, a. Zafra-Gómez, J.I. Vilchez, Non-destructive pigment characterization in the painting little madonna of foligno by X-ray powder diffraction, *Microchem. J.* 134 (2017) 343–353, <https://doi.org/10.1016/j.microc.2017.07.001>.
- [43] S. Bruni, V. Guglielmi, F. Pozzi, Historical organic dyes: a surface-enhanced Raman scattering (SERS) spectral database on Ag Lee-Weisel colloids aggregated by NaClO₄, *J. Raman Spectrosc.* 42 (2011) 1267–1281, <https://doi.org/10.1002/jrs.2872>.
- [44] M. Leona, J. Stenger, E. Ferloni, Application of surface-enhanced Raman scattering techniques to the ultrasensitive identification of natural dyes in works of art, *J. Raman Spectrosc.* 37 (2006) 981–992, <https://doi.org/10.1002/jrs.1582>.
- [45] R. Castro, F. Pozzi, M. Leona, M.J. Melo, Combining SERS and microspectrofluorimetry with historically accurate reconstructions for the characterization of lac dye paints in medieval manuscript illuminations, *J. Raman Spectrosc.* 45 (2014) 1172–1179, <https://doi.org/10.1002/jrs.4608>.
- [46] M.V. Cañamares, M. Leona, Surface-enhanced Raman scattering study of the red dye laccaic acids, *J. Raman Spectrosc.* 38 (2007) 1259–1266, <https://doi.org/10.1002/jrs.1761>.
- [47] F. Pozzi, K.J. Van Den Berg, I. Fiedler, F. Casadio, A systematic analysis of red lake pigments in French Impressionist and Post-Impressionist paintings by surface-enhanced Raman spectroscopy (SERS), *J. Raman Spectrosc.* 45 (2014) 1119–1126, <https://doi.org/10.1002/jrs.4483>.
- [48] G. Germinario, A. Ciccola, I. Serafini, L. Ruggiero, M. Sbroscia, F. Vincenti, C. Fasolato, R. Curini, M. Ioele, P. Postorino, A. Sodo, Gel substrates and ammonia-EDTA extraction solution: a new non-destructive combined approach for the identification of anthraquinone dyes from wool textiles, *Microchem. J.* 1455 (2020) 104780, <https://doi.org/10.1016/j.microc.2020.104780>.
- [49] A. Bosi, G. Peruzzi, A. Ciccola, I. Serafini, F. Vincenti, C. Montesano, P. Postorino, M. Sergi, G. Favero, R. Curini, New advances in dye analyses: in situ gel-supported liquid extraction from paint layers and textiles for SERS and HPLC-MS/MS identification, *Molecules* 28 (2023) 5290, <https://doi.org/10.3390/molecules28145290>.
- [50] V. Beltran, A. Marchetti, G. Nuyts, M. Leeuwestein, C. Sandt, F. Borondics, K. De Wael, Nanoscale analysis of historical paintings by means of O-ptic spectroscopy: the identification of the organic particles in *L'arlésienne (Portrait of madame ginoux)* by van gogh, *Angew. Chem. Int. Edit.* 60 (2021) 22753–22760, <https://doi.org/10.1002/anie.202106058>.